

RESEARCH ARTICLE

Analyzing dwell times with the Generalized Method of Moments

Sadie Piatt, Allen C. Price *

Department of Chemistry and Physics, Emmanuel College, Boston, MA, United States of America

* priceal@emmanuel.edu



Abstract

The Generalized Method of Moments (GMM) is a statistical method for the analysis of samples from random processes. First developed for the analysis of econometric data, the method is here formulated to extract hidden kinetic parameters from measurements of single molecule dwell times. Our method is based on the analysis of cumulants of the measured dwell times. We develop a general form of an objective function whose minimization can return estimates of decay parameters for any number of intermediates directly from the data. We test the performance of our technique using both simulated and experimental data. We also compare the performance of our method to nonlinear least-squares minimization (NL-LSQM), a commonly-used technique for analysis of single molecule dwell times. Our findings indicate that the GMM performs comparably to NL-LSQM over most of the parameter range we explore. It offers some benefits compared with NL-LSQM in that it does not require binning, exhibits slightly lower bias and variance with small sample sizes ($N < 20$), and is somewhat superior in identifying fast decay times with these same low count data sets. Additionally, a comparison with the Classical Method of Moments (CMM) shows that the CMM can fail in many cases, whereas the GMM always returns estimates. Our results show that the GMM can be a useful tool and complements standard approaches to analysis of single molecule dwell times.

OPEN ACCESS

Citation: Piatt S, Price AC (2019) Analyzing dwell times with the Generalized Method of Moments. PLoS ONE 14(1): e0197726. <https://doi.org/10.1371/journal.pone.0197726>

Editor: Miriam R. García, Spanish Council for Scientific Research (CSIC), SPAIN

Received: May 7, 2018

Accepted: December 24, 2018

Published: January 8, 2019

Copyright: © 2019 Piatt, Price. This is an open access article distributed under the terms of the [Creative Commons Attribution License](https://creativecommons.org/licenses/by/4.0/), which permits unrestricted use, distribution, and reproduction in any medium, provided the original author and source are credited.

Data Availability Statement: All scripts and routines for performing the calculations reported in this manuscript, as well as all experimental data used in this work, can be downloaded from <https://sourceforge.net/projects/genmm>.

Funding: This work was funded by the National Science Foundation (www.nsf.gov) RUI Award MCB-1715317 (to ACP) and by Emmanuel College (www.emmanuel.edu). The funders had no role in study design, data collection and analysis, decision to publish, or preparation of the manuscript.

Competing interests: The authors have declared that no competing interests exist.

Introduction

A fundamental challenge in analysis of single molecule data is the determination of the correct model to explain observations. Methods that have been developed to address this fundamental problem include Bayesian inference [1], maximum likelihood [2], as well as Hidden Markov Models (HMM) [3]. Typically, these methods produce a list of dwell times that estimate the time spent in individual molecular states. These dwell times must be analyzed to extract the underlying rates, often using a nonlinear least-squares minimization (NL-LSQM) approach [4]. In this work, we develop and characterize the use of the Generalized Method of Moments for the analysis of dwell times. This method is a statistical estimation method originally developed in econometrics [5].

Single molecule methods generate high resolution quantitative data on biomolecular mechanisms. The advantages of single molecule experiments include identification of rare

intermediates and solution of the “dephasing” problem [6]. In techniques such as single molecule fluorescence, a change in signal level can indicate a state transition. Other methods, such as particle tracking using micro-beads, can also yield data on single molecule rates [7]. The determination of how many states are present and how long the molecule dwells in each state can be challenging, and several methods have been developed to deal with this obstacle [8,9]. Most current methods have focused on analyzing FRET signals, however dwell times can be produced by other methods also, such as bead loss assays [10]. The most common method of analysis, nonlinear least-squares minimization (NL-LSQM), is known to produce biased and non-normally-distributed estimates of the model parameters [4].

The Generalized Method of Moments (GMM) is a powerful statistical method for analysis of samples of random processes. From its original application in the modeling of capital asset pricing [5], its use has grown to make it one of the central methods of econometric analysis [11]. In spite of its broad applicability, its use in the natural sciences has been quite limited, although it has been applied recently to the analysis of simulated stochastic chemical reaction networks [12]. In the GMM, the *population* moments of a random variable, as calculated from a suitable model, are compared to the *sample* moments as calculated from the measured data. Estimates of hidden parameters are determined via minimization of an objective function which quantifies the disagreement between the population and sample moments [11]. The GMM is a general framework that can accommodate a wide range of models and data types. Furthermore, in the limit of a large number of samples, the GMM produces normally-distributed and unbiased estimates [5]. In the method, multiple moments can be considered, each moment resulting in a constraint on the parameters of the model. In the case of under-constrained systems (number of moments less than number of parameters), non-unique solutions exist. When the number of moments is equal to the number of parameters, a unique set of estimates for the parameters can be determined (assuming a real solution exists). This exactly-determined system is often referred to as the Classical Method of Moments (CMM). In the case of an over-constrained system (number of moments greater than the number of parameters), only an approximate solution can be found in general. The GMM is a framework in which all such cases can be handled.

In this work, we develop the application of the GMM to the analysis of single molecule dwell times. We present a general method that can be used to create objective functions applicable to any single molecule experiment that produces dwell times. We characterize the performance of our method by testing it on simulated data. We simulate several common reaction schemes, including single-, double-, and triple-step reactions with both irreversible as well as reversible steps. We have characterized the bias and dispersion of the estimates generated by our method and compared these to the most common alternative method of analysis, NL-LSQM. Additionally, we have collected experimental data on site-specific DNA cleavage by the restriction endonuclease NdeI and analyzed the measured dwell times using our method. Application of the GMM indicates a multistep reaction with fast components independent of protein concentration. The classical method (CMM) is shown to be incapable of analyzing the same data using the multistep models.

Theory

Motivation

More detailed reviews of the GMM can be found in the literature [11]. Here, we review the essentials necessary to understand our work. As motivation, we consider a system with two hidden parameters, a and b , that define a probability density $p(t;a,b)$ for a random variable t .

Define $m_1(a,b) = \langle t \rangle$ and $m_2(a,b) = \langle (t - \langle t \rangle)^2 \rangle$, where the angular brackets indicate the population mean (also known as the expectation value). The population mean of any function $f(t)$ is here defined as

$$\langle f(t) \rangle = \int dt p(t; a, b) f(t). \tag{1}$$

Note that in Eq 1, the population mean has an implicit dependence on the parameters a and b .

These two functions $m_1(a,b)$ and $m_2(a,b)$ are simply the population mean and variance of the random variable t . Now, let \mathbf{t} be a T-dimensional vector whose elements are samples of the random variable t . In this paper, variables in italics represent real numbers and variables in bold represent vectors. The moment functions

$$g_1(a, b, \mathbf{t}, T) = m_1(a, b) - \frac{1}{T} \sum_{i=1}^T t_i \tag{2}$$

and

$$g_2(a, b, \mathbf{t}, T) = m_2(a, b) - \frac{1}{T-1} \sum_{i=1}^T \left(t_i - \frac{1}{T} \sum_{i=1}^T t_i \right)^2 \tag{3}$$

both express the difference between a population moment (first term on the right-hand side) and a sample moment (second term on the right-hand side). Notice that the unbiased estimator is used for the variance (Eq 3). If sample moments give good estimates, then we expect the values on the right-hand sides of Eqs 2 and 3 to be very small for the true values of a and b . A reasonable method would be to set the right-hand side equal to zero and solve for a and b . This method of generating M moment equations for M parameters (in this case $M = 2$) is the Classical Method of Moments (CMM). The CMM has limitations in that there may not be real solutions to the non-linear equations. Additionally, there may be multiple conditions, i.e., moment equations that should be satisfied. In this case, the number of equations may exceed the number of parameters (the over-constrained case), producing an over-constrained system of equations that may have no solution.

General formulation of the GMM

The GMM is a general framework for solving the problems identified in the previous section. In the following derivation, we assume a single random variable. This case generalizes in a straightforward manner to include multi-variate random processes. In our derivation, we assume a probability density for the random variable. It is not strictly necessary that the functional form of the probability density is known. As we will show, our application can be used to determine the *moments* of the distribution without knowing the density. In practice, to relate the moments to questions such as “how many steps are needed to explain this data?” one needs a functional form of the density. Therefore, a single application of this method cannot by itself answer the question “which is the best model to describe this system?” However, comparison of analyses using different models can help with this important problem, as we will show later in this work.

To start, we assume the probability density is a function of the random variable t as well as of n parameters λ and will be written as $p(t; \lambda)$. Note that λ has dimension n . We will also need the joint probability density for multiple independent samples. If we assume there are T samples, this is

$$P(\mathbf{t}; \lambda, T) = \prod_{i=1}^T p(t_i; \lambda). \tag{4}$$

We also need the expectation value of a function of \mathbf{t} . This is defined (analogously to Eq 1) as

$$\langle f(\boldsymbol{\lambda}, \mathbf{t}, T) \rangle = \int d\mathbf{t} P(\mathbf{t}; \boldsymbol{\lambda}, T) f(\boldsymbol{\lambda}, \mathbf{t}, T). \tag{5}$$

In Eq 5, the possible dependence on $\boldsymbol{\lambda}$ and T has been explicitly included.

In order to determine a GMM estimate of the parameters from a given sample, we start with a set of functions, termed generalized moments, such that the expectation value of these functions is zero. That is, we need a set of M functions $g_m(\boldsymbol{\lambda}, \mathbf{t}, T)$ such that $\langle g_m(\boldsymbol{\lambda}, \mathbf{t}, T) \rangle = 0$.

In practice, it is these functions we must assume, not the probability density. However, if we know the probability density, it is straightforward to determine the generalized moments. The index m can assume any value from 1 up to M (the maximum number of moments considered). In general, we may have more moment conditions than parameters ($M > n$), and therefore we can only look for approximate solutions. To do this, the following objective function is minimized with respect to the variables $\boldsymbol{\lambda}$,

$$Q(\boldsymbol{\lambda}, \mathbf{t}, T) = \sum_{m=1}^M \sum_{m'=1}^M W_{m,m'}(\boldsymbol{\lambda}, \mathbf{t}, T) g_m(\boldsymbol{\lambda}, \mathbf{t}, T) g_{m'}(\boldsymbol{\lambda}, \mathbf{t}, T). \tag{6}$$

The matrix $W_{m,m'}$ is a positive definite weight matrix which in general can depend on the parameters $\boldsymbol{\lambda}$ as well as on \mathbf{t} and T . We can understand the form of this objective function by realizing that (1) the function Q is non-negative (due to the positive definite weight matrix), and (2) for large sample size and the true values of $\boldsymbol{\lambda}$, each term $g_m(\boldsymbol{\lambda}, \mathbf{t}, T)$ will be very close to zero. It is then reasonable to expect that minimizing this function over $\boldsymbol{\lambda}$, using some suitable weighting scheme, will produce a good estimate of the true parameter values. The final GMM estimates of the parameters can then be written as

$$\boldsymbol{\lambda}(\mathbf{t}, T) = \arg \min_{\boldsymbol{\lambda}'} Q(\boldsymbol{\lambda}', \mathbf{t}, T). \tag{7}$$

Note that the value of the estimate depends not only on the samples \mathbf{t} and sample size T , but also on the choice of weight matrix $W_{m,m'}$.

When the number of moment conditions M is less than the number of parameters n , this problem is underspecified, and the function Q does not have a unique minimum. If the number of moment conditions is equal to the number of parameters, the system is “just specified,” and, in general, the GMM will give identical estimates as the CMM. This latter point follows since $W_{m,m'}$ is positive definite and therefore $Q \geq 0$. Since the CMM estimates make $g_m = 0$ for all m , we have $Q = 0$ identically and therefore it must be a minimum at that point. It is important to remember that this theorem holds only when the CMM estimate exists (i.e., there are real solutions). Note that it also follows that the just-specified case will be *independent* of the weight matrix $W_{m,m'}$, as the CMM does not use that matrix. In general, for the over-specified case, the GMM estimate does depend on choice of weight matrix, a problem to which we now turn.

In the limit of a large number of samples, the distribution of moments (for fixed parameters), is expected to be Gaussian as a consequence of the Central Limit Theorem. In this case, choosing a weight matrix equal to the inverse of the covariance matrix of the moment functions will lead (in the limit of a large number of samples) to an unbiased estimate of parameters with minimal variance [13]. One should remember that, in general, for finite numbers of samples, the estimate will be biased and not normally-distributed.

To see how this is applied, define the following covariance matrix

$$V_{m,m'}(\boldsymbol{\lambda}, T) = \langle g_m(\boldsymbol{\lambda}, \mathbf{t}, T) g_{m'}(\boldsymbol{\lambda}, \mathbf{t}, T) \rangle. \tag{8}$$

Here, as before, the angular brackets indicate the population mean. Note that since we integrate over the random variables, this covariance matrix is not a function of \mathbf{t} . However, it may

depend on sample size, T . The weight matrix is then the inverse of this matrix:

$$W_{m,m'} = (V^{-1})_{m,m'}. \tag{9}$$

One problem with this approach is that the weight matrix is a function of the parameters λ . This complicates the minimization of the objective function, since the values of these parameters are unknown. Various practical methods of handling this include (1) using the identity matrix for $W_{m,m'}$ (a simple method for getting an initial solution), (2) using various estimates of the covariance matrix calculated from the data itself, (3) using multi-step methods where a simple weighting is used first (often the identity) and then the resulting GMM estimate for the parameters is used to recalculate the weights for a second pass, or (4) continuously updating the weight matrix as the objective function is minimized. With the exception of the continuously updated weight matrix, we will evaluate all of these methods in this work.

Application to single molecule dwell times

The reactions considered will be assumed to be of the type shown in Fig 1. In this figure, states of the system are represented by letters, and the corresponding mean residence times in each state are given by τ_A, τ_B , etc. For the reversible reaction, transition rates are given as k_1, k_2 and k_3 . The observed dwell time is defined as the time it takes the system to enter the final state given that it starts out in state A. For the derivation that follows, we will assume all reactions steps are irreversible. Since the probability density of the total dwell time for a two-step reversible reaction has the same functional form as that of an irreversible scheme, our derivation is applicable to both cases. We will show at the end of this section how to apply our analysis to the reversible two-step reaction. For more than two steps, the functional form of the probability density for reversible schemes is more difficult to relate to our method. We choose to limit ourselves to the irreversible case for more than two steps for two main reasons. First, the theoretical form of the cumulants can be expressed generally and simply, thus allowing a simple and general formulation of a solution. Second, testing n-step irreversible reaction schemes against data is an established method for estimating the number of steps present in experimental data [14,15], thus allowing for application of the cumulant based GMM method to address this question.

The residence time t_A in state A in Fig 1 is drawn from a continuous, single-exponential distribution,

$$p_A(t_A; \tau_A) = \exp\left(-\frac{t_A}{\tau_A}\right), \tag{10}$$

where τ_A is the mean dwell time in state A. A similar function can be defined for state B, C, etc. The mean observed dwell time for the system is therefore

$$\langle t \rangle = \tau_A + \tau_B + \dots + \tau_E. \tag{11}$$

Since each step is independent and exponentially-distributed, the population variance is given by an analogous formula,

$$\langle t^2 \rangle - \langle t \rangle^2 = \tau_A^2 + \tau_B^2 + \dots + \tau_E^2. \tag{12}$$

In order to formulate a general method for these systems, we would like a formula analogous to Eq 12 for higher order moments. We can find such a generalization with cumulants. For any random process which is a sum of independent random processes, the m^{th} order cumulant is merely the sum of the m^{th} order cumulants of the individual processes. In this case, if we

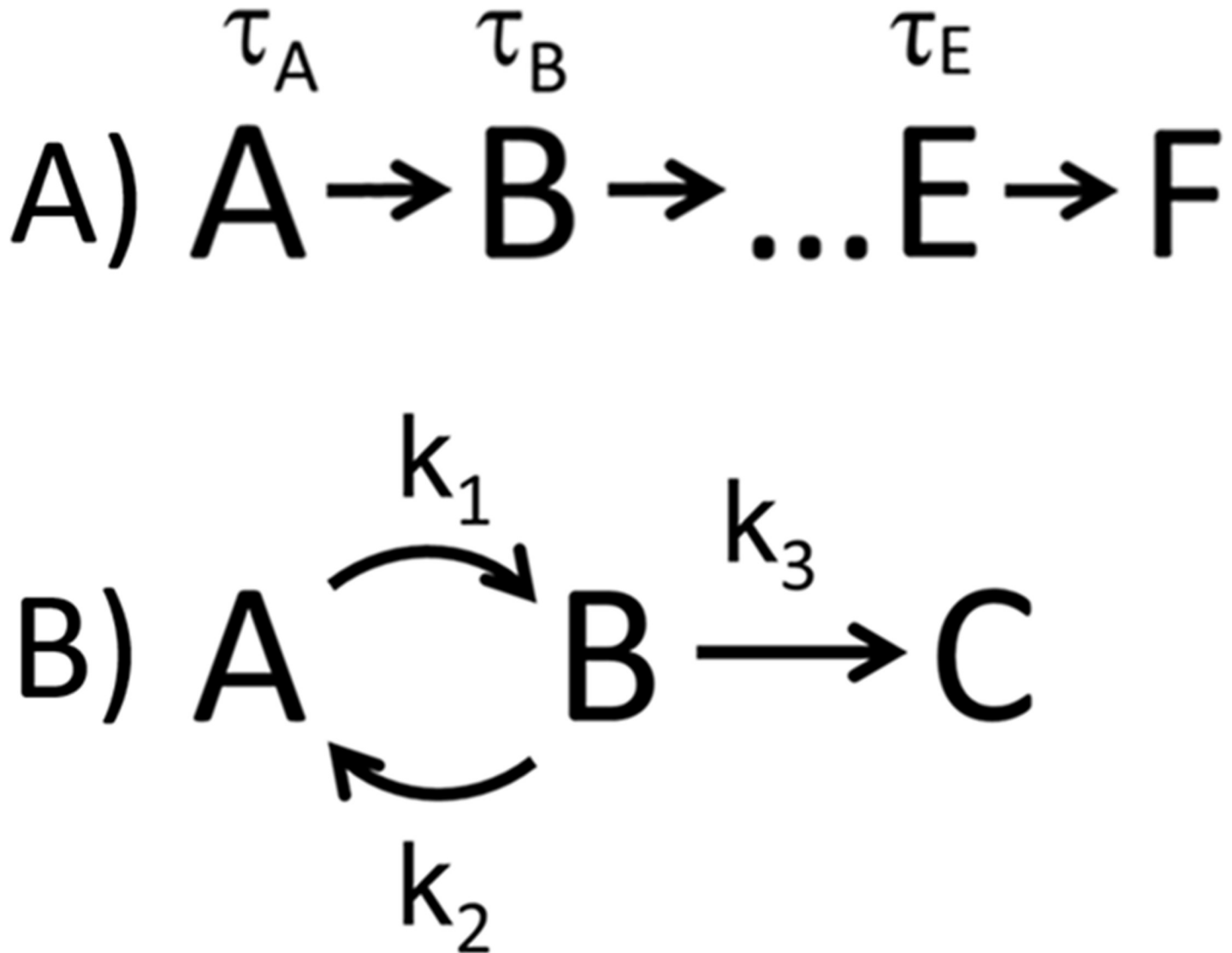


Fig 1. Reaction schemes. Each state is represented by a letter and the mean residence time in that state is τ_A , τ_B , etc. (A) The n -step irreversible reaction scheme. (B) The two-step reversible scheme. The transition rates in the reversible reaction are given by k_1 , k_2 , and k_3 .

<https://doi.org/10.1371/journal.pone.0197726.g001>

represent the cumulant of the total dwell time with $\kappa^{(m)}$, then we have

$$\kappa^{(m)} = \kappa_A^{(m)} + \kappa_B^{(m)} + \dots + \kappa_E^{(m)}. \tag{13}$$

In this equation, $\kappa_A^{(m)}$ is the m^{th} order cumulant of step A, etc. The m^{th} order cumulant for an exponential distribution is

$$\kappa_A^{(m)} = (m - 1)! \tau_A^m, \tag{14}$$

which allows us to write the general formula for the cumulants for an n -step irreversible reaction scheme.

$$\kappa^{(m)} = (m - 1)! (\tau_A^m + \tau_B^m + \dots + \tau_E^m). \tag{15}$$

Eq 15 gives the population cumulants of the reaction scheme shown in Fig 1. In order to

complete the moment function, we need to calculate unbiased estimates of the cumulants from the measured samples. Formulas for unbiased sample cumulants exist and are referred to as k -statistics [16]. In order to define the k -statistics for this problem, let us first define the l^{th} order central moments.

$$m_1 \equiv \frac{1}{T} \sum_{i=1}^T t_i, \tag{16}$$

$$m_l \equiv \frac{1}{T} \sum_{i=1}^T (t_i - m_1)^l, \quad l > 1. \tag{17}$$

The k -statistics up to order 4 are then

$$k^{(1)}(\mathbf{t}, T) = m_1, \tag{18}$$

$$k^{(2)}(\mathbf{t}, T) = \frac{T}{T-1} m_2, \tag{19}$$

$$k^{(3)}(\mathbf{t}, T) = \frac{T^2}{(T-1)(T-2)} m_3, \tag{20}$$

$$k^{(4)}(\mathbf{t}, T) = \frac{T^2}{(T-1)(T-2)(T-3)} [(T+1)m_4 - 3(T-1)m_2^2]. \tag{21}$$

Note that the first and second order expressions are the usual definitions of the sample mean and sample variance in the random variable t .

We can now state our m^{th} order generalized moment function for the n -step reaction.

$$g_m(\tau_A, \tau_B, \dots, \mathbf{t}, T) = \kappa^{(m)}(\tau_A, \tau_B, \dots, \tau_E) - k^{(m)}(\mathbf{t}, T) \tag{22}$$

In this expression, the population cumulant $\kappa^{(m)}$ is given by Eq 15 above, and the term $k^{(m)}$ is to be an unbiased estimate of the cumulant as calculated from Eqs 18–21.

The GMM is not completely defined until the weight matrix is specified. We evaluate several options in this paper. These include the identity matrix, the inverse of a jackknife estimate of the covariance matrix, and the inverse of a covariance matrix calculated using a Monte-Carlo method. We leave the description of these methods to the Materials and Methods section of this paper. Eqs 15–21 completely define the moment functions used in this study. They, along with the weight matrix, define the GMM for this problem.

The case of a reversible two-step reaction

For a two-step reaction, such as those shown in Fig 1, the total dwell time can be shown to obey a probability density of the following form [14],

$$p(t; \tau_A, \tau_B) = \begin{cases} \frac{\exp(-t/\tau_A) - \exp(-t/\tau_B)}{\tau_A - \tau_B} & \tau_A \neq \tau_B \\ \frac{t}{\tau^2} \exp(-t/\tau) & \tau = \tau_A = \tau_B \end{cases}. \tag{23}$$

In the case of a reversible first step, the decay constants will be equal to

$$\frac{1}{\tau_{B/A}} = \frac{1}{2} (k_1 + k_2 + k_3) \pm \sqrt{\frac{1}{4} (k_1 + k_2 + k_3)^2 - k_1 k_3}. \tag{24}$$

In this equation, the plus sign applies to τ_B and the minus sign to τ_A . The GMM described in this work will determine estimates for the parameters τ_A and τ_B , which can be related to the underlying rate constants in the reversible reaction model by Eq 24.

Materials and methods

Simulations and GMM calculations

Dwell times were simulated for multistep stochastic reactions by adding samples individually drawn from exponentially-distributed random processes. The sets of decay parameters used were as follows. For the single-step, all trials used a decay time of 10 s. For the two-step reaction, decay parameters pairs used were (10 s, 10 s), (10 s, 20 s), (10 s, 50 s) and (10 s, 100 s). For the three-step reaction, decay parameters sets were (10 s, 10 s, 10 s), (10 s, 10 s, 50 s), and (10 s, 30 s, 100 s). For all decay parameter sets, sample sizes used were 5, 10, 20, 50, 100, 200, 500 and 1000. For each set of parameters and sample size, 1000 trials were simulated. For each trial, unbiased estimates of cumulants were calculated using k -statistics up to 4th order.

Four different weight matrices were evaluated. These were (1) the identity matrix, (2) a diagonal matrix with elements equal to the inverse of a jackknife estimate of the variance of the cumulants, (3) the matrix inverse of a jackknife estimate of the covariance matrix of the cumulants, and (4) the inverse of an interpolated covariance matrix. All jackknife estimates were determined from a single trial in the following manner. First, N subtrials were created by sequentially removing each sample from the trial (resulting in N subtrials of $N-1$ samples each). Then, these N subtrials were used to calculate N distinct estimates of the cumulants. Finally, the variance or covariance was calculated from these estimated cumulants and the result was scaled by $(N-1)/N$. The interpolated covariance was calculated by linear interpolation from a set of previously-calculated covariance matrices. These previously-determined matrices were calculated using a Monte Carlo (MC) method for a wide range of values of N (sample size) and decay parameters (τ_A , τ_B , etc.). For the MC calculations, 10^5 trials were calculated, and the covariance was calculated directly from the cumulants of these trials.

The objective function (Eq 6) was minimized using the Broyden-Fletcher-Goldfarb-Shanno algorithm with an explicit gradient. Global minima were found by using a logarithmically-spaced grid of initial trial points. The parameter space region searched was an 'n-cube,' where n is the number of parameters (the number of steps in the reaction). The grid spacing was a factor of ten. For example, for a two-step reaction, the two-dimensional region $[1, 1000] \times [1, 1000]$ was searched. This included starting points an order of magnitude less and more than the minimum and maximum decay parameters simulated. Note that since the GMM objective functions examined here are multi-polynomials of the decay parameters, the minimization is robust, as the surface is not rough (i.e. it does not exhibit a large number of minima). In the two-pass GMM, the estimates for the decay parameters from a first-pass minimization were used as the starting search point for a second pass which used the interpolated weight matrix calculated from the first pass parameter estimates.

All scripts and routines for performing the calculations reported in this manuscript, as well as sample data sets, can be downloaded from <https://sourceforge.net/projects/genmm>. These scripts are not intended to be end user software, but are made available to encourage transparency, reproducibility and to encourage others to build on our work.

Nonlinear least-squares minimization

To perform the NL-LSQM of the simulated data, each simulated data set was binned into a number of bins equal to the square root of the number of samples (rounding up to the nearest

whole number). The bins were fit to a bi-exponential distribution with two free decay parameters using the Levenberg-Marquardt algorithm. A finite bin-width correction was used.

Experimental data collection and processing

Experimental dwell times were measured for DNA cleavage by the restriction endonuclease NdeI. The method of data collection is explained in detail elsewhere [10]. Briefly, 1000 bp DNAs with a single centrally-located NdeI restriction site were used to tether 1 μm magnetic beads in a microflow channel. The DNA-tethered beads were observed under low magnification and dark field imaging. A low flow rate and magnet were used to apply a small force (<100 fN) to the beads, which are pulled out of focus as the DNA is cleaved. Varying concentrations of NdeI (from 25 to 350 pM) were introduced in reaction buffer (20 mM Tris-HCl, 100 mM NaCl, 3 mg/mL BSA, 1 mg/mL Pluronic F-127, 1 mM MgCl_2). Dwell time between initial introduction of the enzyme and the final cleavage of the DNA is measured by noting the time at which the bead is removed. The software package ImageJ was used to locate bead positions in the initial image, and then all images were analyzed by custom software which integrates the intensity around the bead position. A large drop in intensity identifies the cleavage event, and the dwell time is recorded as the frame number. A frame rate of either 0.5 or 1 fps was used. Individual data sets produced 200 to 700 dwell times (cleavage events). See Section 12 of [S1 Supporting Information](#) for histograms of experimental data. This data is available for download from <https://sourceforge.net/projects/genmm>. Mean dwell times varied from 150 s to 300 s, and data were analyzed using the GMM. One up to six step reaction models were tested using the “just-specified” objective function for each scheme. A single pass GMM was used.

Results

Performance of GMM with simulated data

By minimizing an objective function composed of moment functions, the GMM provides estimates of parameters which approximately satisfy the condition that all the moment functions have the value zero. The performance of the GMM is known to depend on the order of the method (the number of moment conditions included), as well as on the nature of the weighting matrix used to weight the various terms. In addition, various methods of weighting have been developed. These include “two-pass” methods, in which an initial trail matrix is used to find a first pass estimate. The second pass uses a more effective weight matrix calculated from the results of the first pass.

In general, we found a diagonal weight matrix based on jackknife estimates of the variances in the cumulants (the D-matrix) to produce estimates with the lowest bias for all orders. [Fig 2](#) shows the results of analyzing simulated data for a single-step reaction. Most methods of analysis do well with a single-step mechanism. We include the analysis here for completeness and because it displays trends which also hold for the more complicated mechanisms. The results are shown for methods of all orders up to fourth. The dispersion in the results is shown by representing the mean deviation with error bars. The identity matrix (I-matrix) as well as a non-diagonal matrix based on a jackknife estimate of the full covariance matrix of the cumulants (C-matrix) gave poorer results.

As seen in [Fig 2](#), the bias and dispersion reduce with increasing number of samples for all orders (except for first order where the bias is zero). Additionally, the bias tends to increase as the order of the method is increased for all sample sizes. Note that the first order method is equivalent to the Classical Method of Moments, in which the estimate is simply the mean of the sample dwell times. It is easily shown that this estimate is unbiased for all sample sizes. We

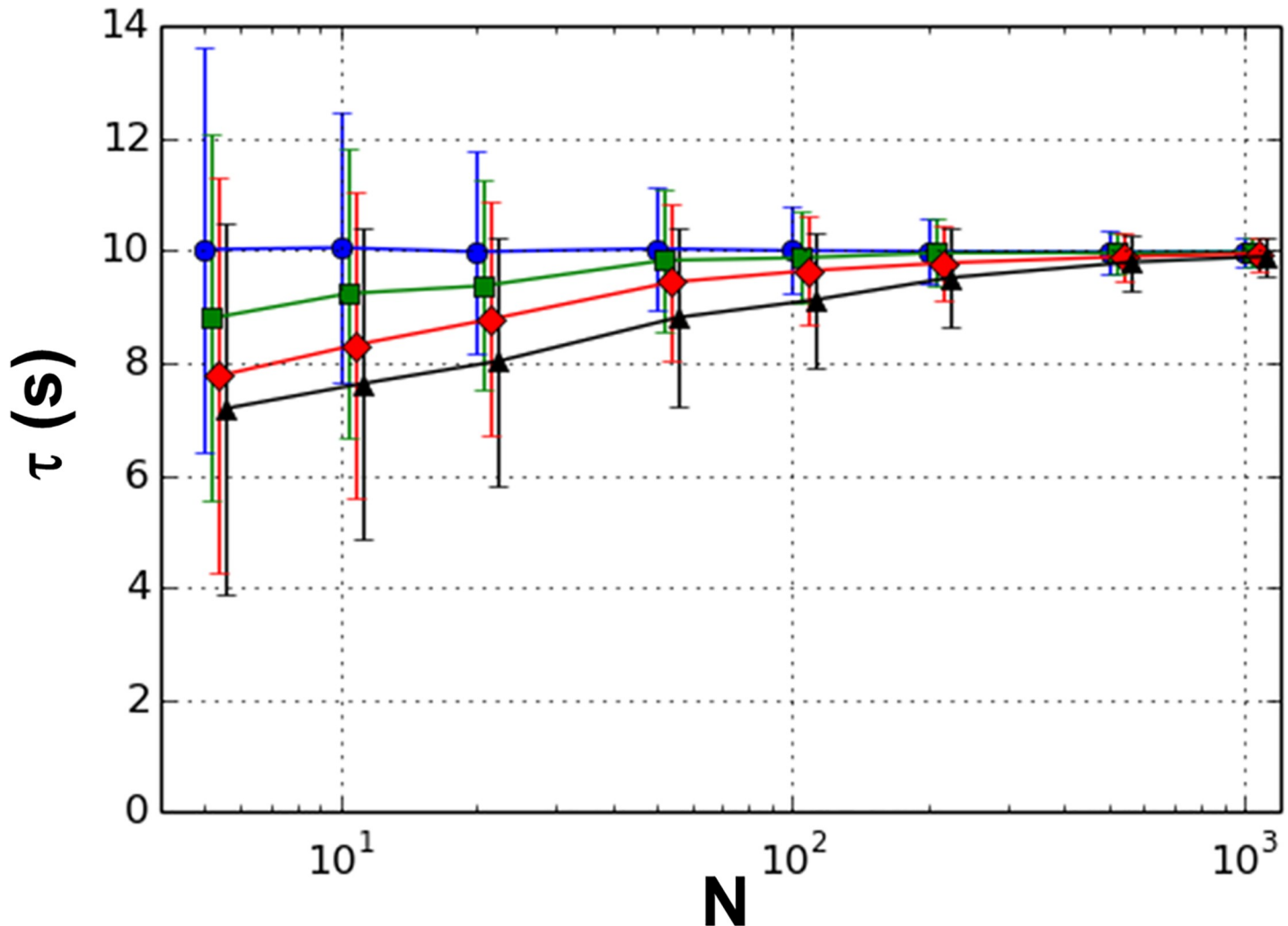


Fig 2. Results for 1 step reaction. Mean for 1000 trials for orders 1 (circles), 2 (squares), 3 (diamonds), and 4 (triangles) are plotted versus sample size (N). The simulated decay constant is 10 s. Error bars represent mean deviations.

<https://doi.org/10.1371/journal.pone.0197726.g002>

found that the dispersion, as measured by the mean deviation, shows a complex dependence on the order of method for the I-matrix. However, for the D- and C-matrices, the dispersion is relatively independent of order.

We now turn to the performance of the GMM for the two-step reaction (a single intermediate). In all that follows, we hold the first decay parameter fixed ($\tau_A = 10$ s) and vary the second ($\tau_B = 10, 20, 50,$ or 100 s). We examined second, third, and fourth order methods. Note that in this case, the first order method is under-constrained, does not result in a unique estimate, and is therefore excluded. We also examined the effect of using the I-, D-, and C-matrices (defined above), as well as the benefit of a two-pass GMM, in which a first pass estimate is used to recalculate the weight matrix.

For the two-step reaction model, the GMM returns two estimated decay parameters which can be sorted into a smaller value and a larger value. We can clarify the relation between these two returned parameters and the hidden parameters τ_A and τ_B by considering the form of Eqs 14, 15 and 22. The first order moment function only depends on the sum of the two decay parameters. By a reparameterization, we can make the first moment function dependent on a

single parameter which is equal to the sum of all decay parameters. In the case of the just-specified system, we can always find parameters to make each moment term zero, and hence any solution will have the sum of the two estimates equal to an unbiased estimate of the mean total dwell time. For the over-constrained case, the sum will not be unbiased. For the reversible reaction, one can see by Eq (24) that the sum of the returned estimates will be the inverse of the sum of all the reaction rates.

In Fig 3, we plot the mean values of the two estimates, along with the mean deviations as error bars, for two sets of model parameters, $(\tau_A, \tau_B) = (10 \text{ s}, 10 \text{ s})$ and $(\tau_A, \tau_B) = (10 \text{ s}, 50 \text{ s})$. The results shown were calculated using the D-matrix, which gave the best results for these trials (see Sections 1–6 in [S1 Supporting Information](#) for complete results). The bias and dispersion decrease with increasing sample size, consistent with the expected large sample size behavior [5]. For the case of $\tau_B = 50 \text{ s}$ (Fig 3C and 3D), we see that for both estimates, bias *increases* with order, similar to the pattern for the one-step reaction. However, the sign of the bias is different for the two estimates, such that the lower estimate is too high, and the higher estimate is too low. Dependence of the dispersion on the order is either weak or shows a slight increase as order goes up. Results for decay parameters $\tau_B = 100 \text{ s}$ are similar to those for $\tau_B = 50 \text{ s}$ (see Sections 1–6 of [S1 Supporting Information](#)).

For the case when both model parameters are equal ($\tau_A = \tau_B = 10 \text{ s}$), the bias is either independent of order (Fig 3A) or shows a non-trivial dependence on order and sample size (Fig 3B). Results for decay parameters $(\tau_A, \tau_B) = (10 \text{ s}, 20 \text{ s})$ are intermediate between those for $\tau_B = 10 \text{ s}$ and $\tau_B = 50 \text{ s}$ (see Sections 1–6 of [S1 Supporting Information](#)). The above results indicate that a second-order method using the D-matrix is the optimum method of those explored using the parameters we tested.

We next tested the two-pass GMM on the simulated data. Two-pass GMM methods attempt to generate a more accurate weight matrix by executing a first pass using a best guess for the weight matrix, and then using the resulting first pass estimates to calculate a more accurate weight matrix for the second pass. In our case, we chose our best single-pass GMM result (the second order, D-matrix method) as our first pass. We then used the estimates from this pass to calculate the theoretical covariance in the sample cumulants and from the inverse of this, the weight matrix. For efficiency, the theoretical covariance was calculated by interpolation from a set of covariance matrices that were calculated using a Monte Carlo method (see [Materials and Methods](#) for details). Since the second order GMM is “just-specified” in the case of two model parameters, and hence independent of weight matrix, we investigated the effect of adding a second pass using up to third or fourth order moments.

The results from the two-pass GMM are shown in the Fig 4. As can be seen from the figure, an additional pass does not greatly affect the bias nor the dispersion under any of the parameter sets used in this study. The small reduction in bias seen at low sample numbers in Fig 4A and 4D is offset by the small increase in bias shown in Fig 4B and 4C. Fig 4 only shows the results from the D-matrix weighting scheme. See Section 7 of [S1 Supporting Information](#) for complete results.

We additionally applied the GMM to a three-step reaction model. Third and fourth order single-pass GMM methods were applied to three sets of decay parameters. These sets were $(\tau_A, \tau_B, \tau_C) = (10 \text{ s}, 10 \text{ s}, 10 \text{ s})$, $(10 \text{ s}, 10 \text{ s}, 50 \text{ s})$ and $(10 \text{ s}, 30 \text{ s}, 100 \text{ s})$. GMM estimates were sorted into smallest to largest returned value, and the means and mean deviations are shown in Fig 5. The performance of the GMM estimation is quite varied when faced with this more challenging problem. Bias tends to decrease with increasing sample number for most estimates, except for the lowest estimate for the case of parameters (10s, 10s, 50s). This increase in bias with sample number is surprising, and therefore for the (10s, 10s, 50s) simulated data, we extended the analysis up to 10^4 samples. The results (see Section 9 of [S1 Supporting Information](#)) show that

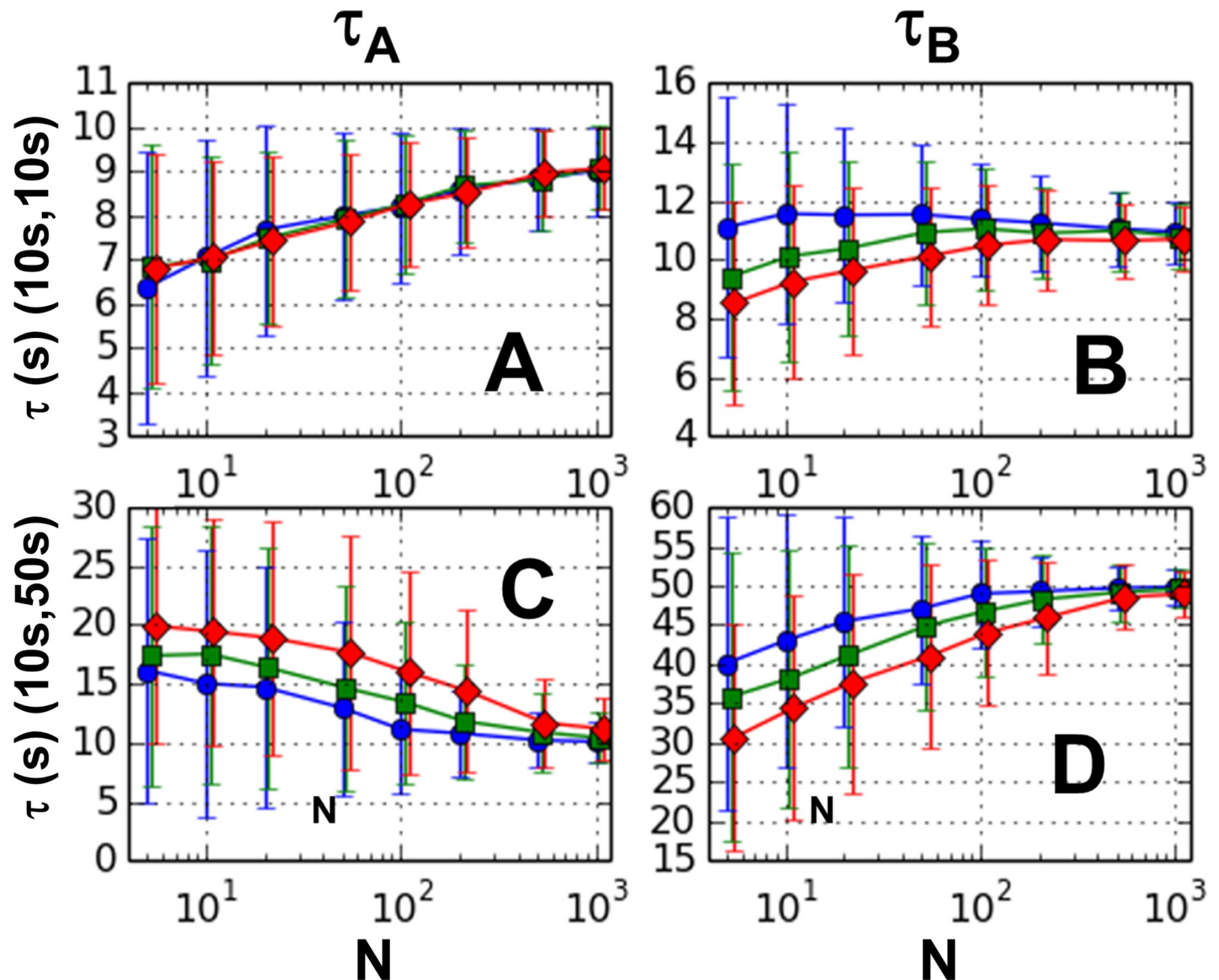


Fig 3. Single pass GMM results for 2 step reaction. Means for 1000 trials for orders 2 (circles), 3 (squares), and 4 (diamonds) are plotted versus sample size (N). Error bars represent mean deviations. Left panels (A and C) show lower estimate and right panels (B and D) show higher estimate. The two top panels (A and B) are for the decay constant pair (10 s, 10 s) and the two bottom panels (C and D) for (10 s, 50 s).

<https://doi.org/10.1371/journal.pone.0197726.g003>

the bias in the lowest returned parameter eventually begins to reduce for large enough samples (~ 500 samples for 3rd order, ~ 1000 for 4th order).

Comparison with NL-LSQM

In order to compare the GMM to alternative methods, we used a non-linear least squares minimization (NL-LSQM) method based on fitting histograms of our simulated two-step reaction data to the theoretical bi-exponential distribution. We used the same simulated data that was used to calculate the GMM estimates shown in Fig 3 and performed global nonlinear least-squares minimizations as described in the Materials and Methods. Fig 6 shows a comparison of the second order GMM method using the D-matrix to the NL-LSQM method for a two-step

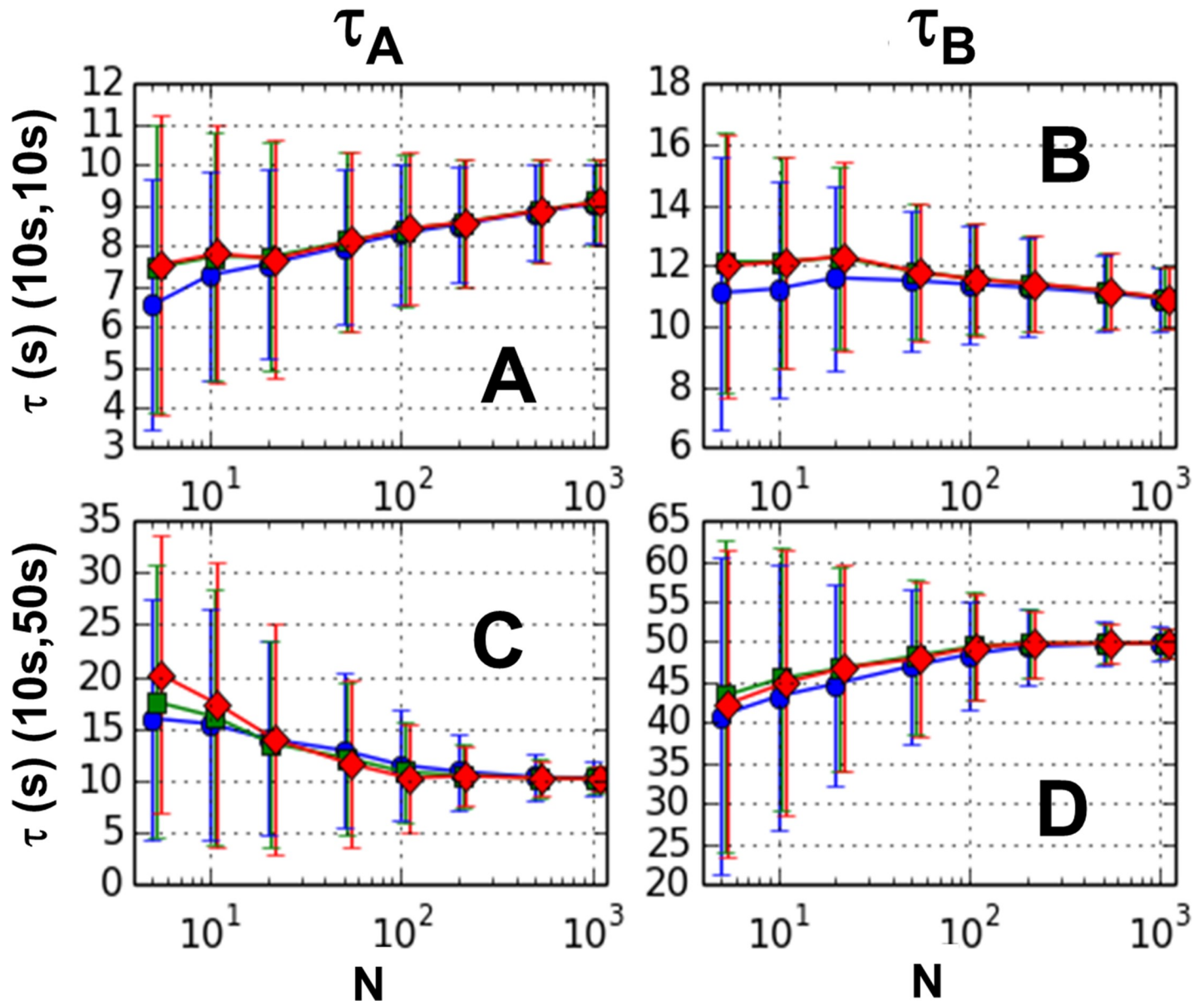


Fig 4. Two pass GMM results for 2 step reaction. Mean for 1000 trials for one-pass 2nd order (circles), two-pass 3rd order (squares), and two-pass 4th order (diamonds) is plotted. Error bars represent mean deviations. Left panels (A and C) show lower estimate and right panels (B and D) show higher estimate. The two top panels (A and B) are for the decay constant pair (10 s, 10 s) and the two bottom panels (C and D) for (10 s, 50 s).

<https://doi.org/10.1371/journal.pone.0197726.g004>

reaction. Note that for sample sizes of 5 and 10, the NL-LSQM method showed very large bias for the smaller decay parameter (in some cases, returning negative decay parameters) which is not plotted. For large samples ($N > 100$) the two methods are comparable in bias and dispersion, except for the case where the two model parameters are equal, in which case the GMM has slightly smaller bias. At low sample size ($N < 20$), the GMM shows less bias and dispersion and is able to return reasonable estimates even for sample sizes as small as $N = 5$. Results for the decay parameter pairs (10s, 20s) and (10s, 100s) are shown in Section 8 in [S1 Supporting Information](#).

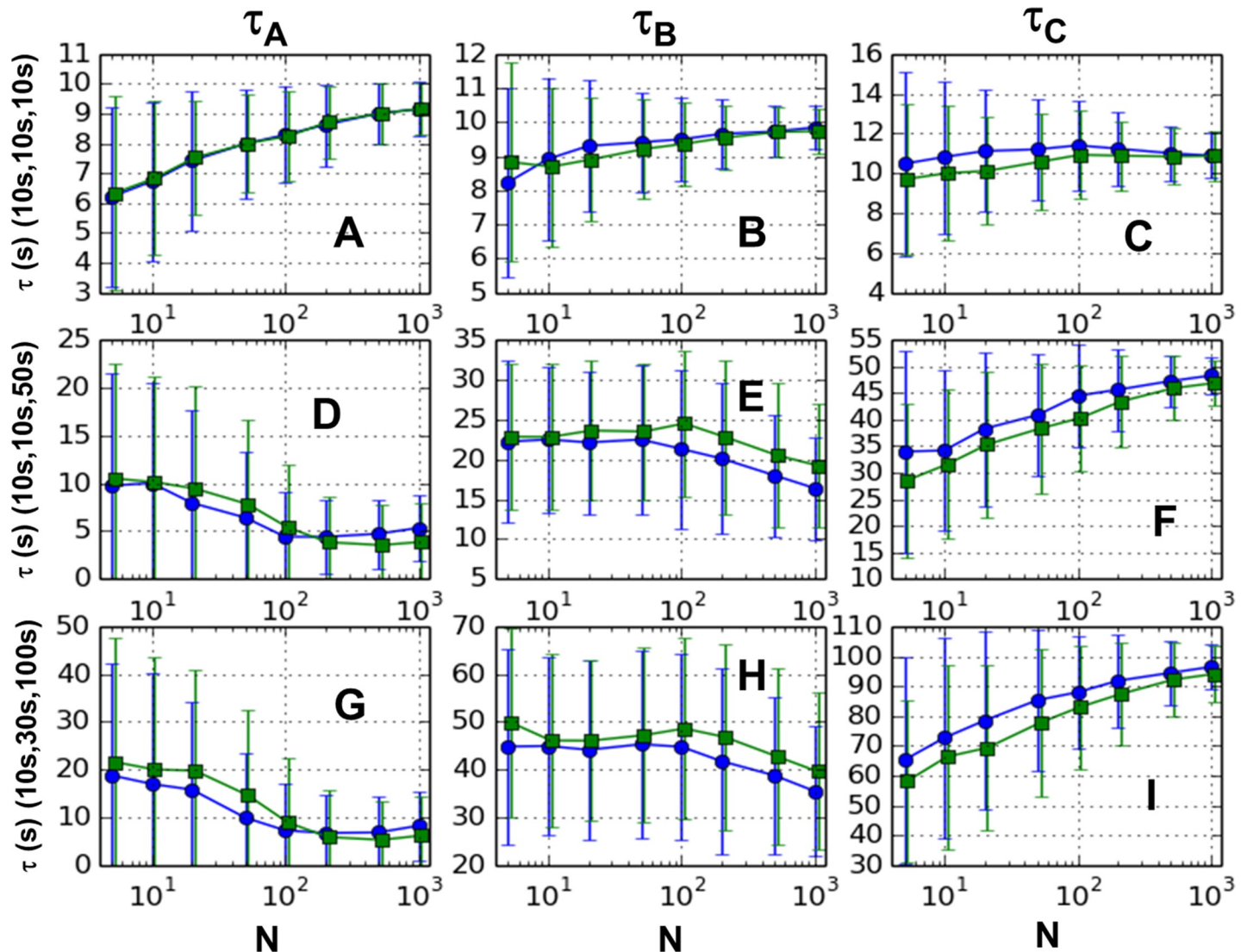


Fig 5. Single pass GMM results for 3 step reaction. Mean for 1000 trials for orders 3 (circles) and 4 (squares) versus sample size (N). Error bars represent mean deviations. The three GMM estimates are sorted into smallest to largest and arranged left to right in each row. Top panels (A, B, & C) are for the decay constants (10s, 10s, 10s), middle panels (D, E, & F) for (10s, 10s, 50s), and bottom panels (G, H, & I) for (10s, 30s, 100s).

<https://doi.org/10.1371/journal.pone.0197726.g005>

Application to experimental data

To gain experience using the GMM with experimental data, we collected single molecule data of double stranded DNA cleavage using a bead loss assay we have previously described [10]. Single molecule dwell times of DNA cleavage have been shown to be useful for the study of restriction endonuclease mechanism [17]. Our technique uses tethered beads to measure the dwell time until cleavage for several hundred DNAs in a single experiment. The total dwell time consists of several steps, including the DNA target search as well as the cleavage of each strand of the DNA.

We have previously shown that the mean dwell time under the conditions of 2 mM Mg^{2+} is highly dependent on protein concentration, consistent with a diffusion-controlled process. In this work, we collected data at 1 mM Mg^{2+} for a range of concentrations from 25 pM to 350 pM (see Section 12 of [S1 Supporting Information](#) for histograms of data) and analyzed the

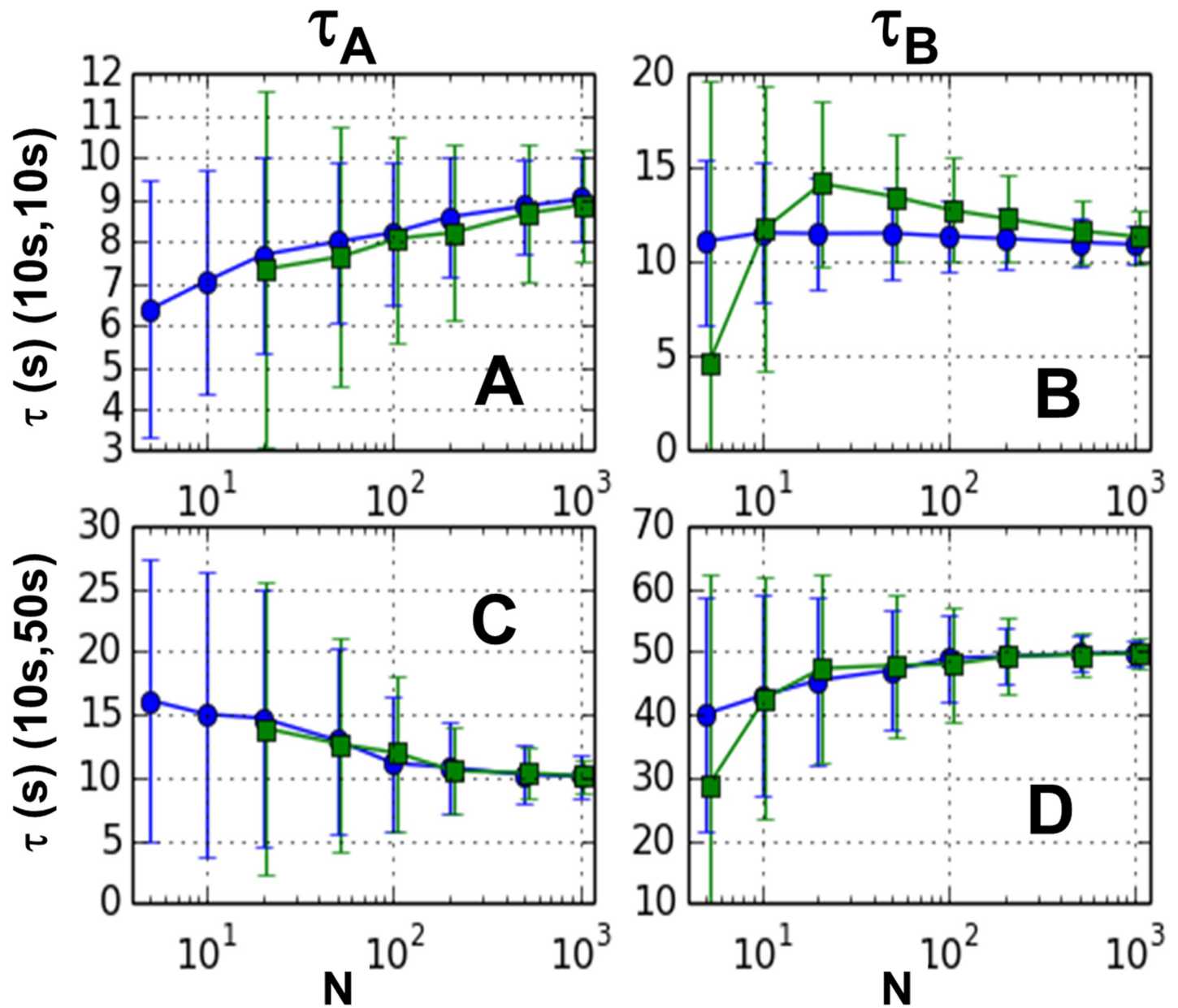


Fig 6. Results for comparison of GMM to non-linear least squares. Estimates from GMM are shown in blue circles, and those of NL-LSQM are green squares and are plotted versus sample size (N). Error bars represent mean deviations. Left panels (A and C) show lower estimate and right panels (B and D) show higher estimate. The two top panels (A and B) are for the decay constant pair (10s,10s) and the two bottom panels (C and D) for (10s, 50s).

<https://doi.org/10.1371/journal.pone.0197726.g006>

resulting dwell times using the GMM. Since we did not know *a priori* the number of steps in the reaction, we chose to test models with one up to six steps, each using the “just-specified” order (i.e., first order for one-step, second order for two-step, etc.) and using a diagonal jack-knife weight matrix (D-matrix).

Our results for the one- and two-step analysis are shown in Fig 7. The single-step result is equal to the sum of the two decay times from the two-step analysis, which must be the case. The results for the three- and four- step method are listed in Table 1. Examination of the graph and table shows that the slowest time step remains relatively constant for the different models

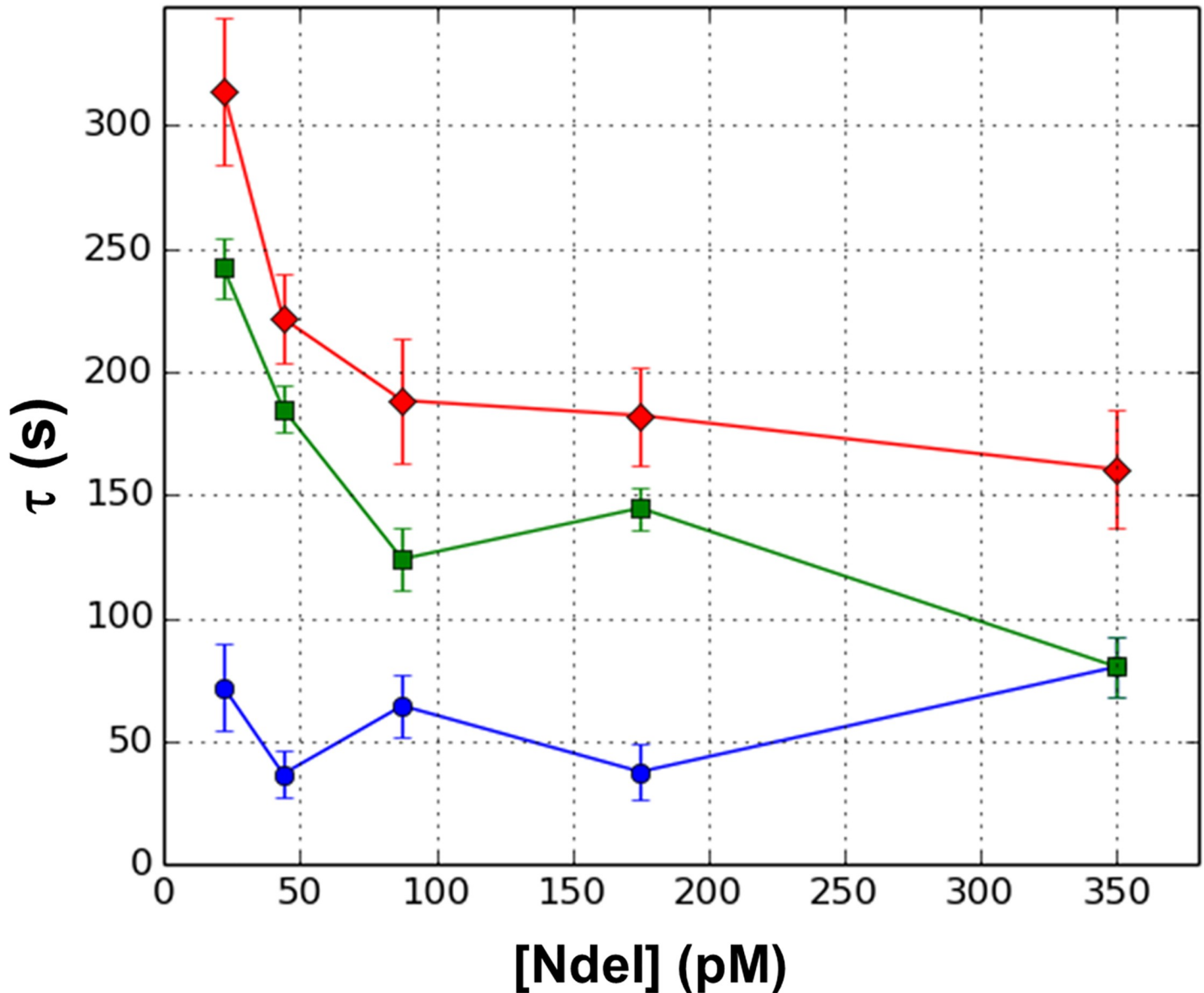


Fig 7. Application of GMM to DNA cleavage by NdeI. All results are for single-pass GMM. The results for one-step reaction, first order GMM are shown with red diamonds. Results for a two-step reaction, second order GMM are shown in green squares and blue circles. Error bars are estimates of statistical uncertainty taken from dispersion shown in Fig 3.

<https://doi.org/10.1371/journal.pone.0197726.g007>

as we increase the number of steps in the model past two. For example, at 22 pM, the slowest step in the two-step model is 242 s, which changes to 259 s in the three-step model, and then 265 s in the four-step model. But the faster steps show a different pattern. For this same data, the two-step model yields a faster step of 72.0 s, which turns into two steps of 27.5 s in the three-step reaction, and finally three steps of 16.4 s in the four-step. Note that in each model, the sum of the faster steps is relatively constant. This pattern continues for the five- and six-step models also.

The fact that the higher order GMM yields sets of identical parameters suggests that the CMM might not give real solutions for these data sets (see Section 11 of [S1 Supporting Information](#)). We tested this by applying the CMM method to our experimental data. In this

Table 1. Results of three and four step GMM analysis of experimental data.

[NdeI] (pM)	THREE STEP RESULTS			FOUR STEP RESULTS			
	τ_1 (s)	τ_2 (s)	τ_3 (s)	τ_1 (s)	τ_2 (s)	τ_3 (s)	τ_4 (s)
22	27.5	27.5	259	16.4	16.4	16.4	265
44	11.1	11.1	199	5.05	5.05	5.05	206
88	21.4	21.4	145	12.4	12.4	12.4	151
175	11.8	11.8	159	5.96	5.96	5.96	164
350	36.3	36.3	91.9	21.6	21.6	21.6	99.7

Protein concentration is listed in left hand column. The decay times for the GMM results are listed in order of increasing time. The time for the slowest step is in the rightmost column under each model result.

<https://doi.org/10.1371/journal.pone.0197726.t001>

method, the moment conditions (defined by Eq 2) are set identically to zero up to the n^{th} order, where n is the number of steps in the reaction model. These equations were solved numerically using Mathematica. At first order, the CMM gives identical results to the GMM, as expected. At second order, the CMM gives identical results for all data sets except for the 350 pM data set, for which the GMM returns two identical time steps. For the 350 pM data set, the CMM returns two complex solutions. This is also expected, as the GMM returns a double root when the CMM does not yield real solutions (see Section 11 of [S1 Supporting Information](#)). For all higher orders, the CMM failed to return a complete set of real solutions. In all cases, the CMM returned at most two real values, with some of these negative. The real CMM estimates did not in general show any relation to the GMM results. Clearly, the CMM is not able to provide useful parameters for this experimental data.

We also considered the possibility that the data might contain time steps that were significantly different and that the GMM might have trouble analyzing such data. To test this, we simulated three-step data with time steps of (1s, 10s, 100s) as well as (1s, 20s, 400s). The results of such numerical experiments are shown in Section 10 of [S1 Supporting Information](#). The performance of the GMM is similar to what we saw for the previously considered case of (10s, 30s, 100s) and does not show behavior similar to the experimental case.

To further test how the GMM would handle data that contained multiple steps, we generated two simulated test datasets, one of a two-step reaction with time steps (50s, 150s), and one of a six-step reaction with time steps (10s, 10s, 10s, 10s, 10s, 150s). We then applied the just-specified GMM (single pass) using different numbers of steps (one up to six) in the model. For the two-step data, we found that as we increase the number of steps in the model, the method returned negative time constants when asked for more than two steps. The greatest returned decay times were relatively constant and close to (50s, 150s), indicating that even when we choose to analyze the data with the incorrect model, the method was correctly identifying the steps present in the data and then returning insignificant durations for the fictitious steps. For the six-step simulated data, the largest time constant remained relatively constant and close to the expected value of 150s. The faster decay constants were all much smaller but varied quite a bit, and the algorithm began to return negative time constants when more than four steps were assumed in the model. This shows that the method could not correctly identify the number of fast steps but did seem to suggest that there were at least four. This is similar to what we observed in the analysis of our data, and suggests that in our experimental system, there are several fast steps and one slower one. This slow step is shown by the green curve in [Fig 7](#) and the faster decays are represented by the blue curve in [Fig 7](#), whose value is the sum of the faster decays.

Discussion

We have developed an application of the Generalized Method of Moments (GMM) to the analysis of single molecule dwell times. Originally developed for the analysis of econometric data, the GMM is a statistical framework for the analysis of samples drawn from random processes. Our method is based on the analysis of cumulants of the data, and we have shown that it can be used successfully to analyze single molecule biophysical data. Using simulated as well as experimental data, we have shown that the GMM can extract useful model parameters directly from sets of experimentally-measured dwell times. We also provide guidelines on the best use of the GMM to analyze real data.

Many of our findings agree with the growing literature assessing the utility of the GMM. Our simulated data shows that for applications to single molecule dwell times, the lowest order method that can completely determine a solution (the “just-specified” case) demonstrates lower bias than higher order methods. For orders higher than this minimum, the bias generally depends on the nature of the weight matrix. In the two-step reaction, we investigated the effect of three different weight matrices for these higher order GMMs. These were (1) the identity matrix, (2) a diagonal weight matrix with terms equal to the inverses of estimated variances of the cumulants, and (3) a matrix equal to the inverse of an estimated covariance matrix. We find that, although estimating the variances of the cumulants from the data can reduce bias, adding more complicated weight matrices (including off-diagonal terms due to cross-variances) can actually *increase* bias. These results indicate a “less-is-more” approach. Adding higher orders or off-diagonal elements to the weight matrix does not necessarily help the estimate. We also found that adding a second pass does not significantly improve performance.

Even under “just-specified” constraints, i.e., when the number of moment conditions equals the number of free parameters, our results for the two-step reaction shows dependence on weight matrix, albeit small (See Section 4 of [S1 Supporting Information](#)). Although it is true that the just-specified GMM method generally gives the same results as the Classical Method of Moments (CMM), this only follows if the CMM returns a real-valued result. In the case of the two-step reaction, it is straightforward to show that the CMM fails to return real-valued estimates in many cases. In these cases, the GMM will return real values that *depend* on the weight matrix. Furthermore, it can be shown that in the cases in which the CMM does not return real-valued estimates, the second order GMM must return a *double root*, that is, it returns two identical estimates (see Section 11 of [S1 Supporting Information](#) for proof of this statement). Since these estimates tend to be midway between the higher and lower decay constants, they have the effect of causing the higher estimate to have *negative* bias and the lower estimate to have *positive* bias, a trend which is seen in our simulated data (Figs 3 and 4). It is worth noting that other methods of dwell time analysis, including Bayesian methods and Hidden Markov Models, have been shown to systematically underestimate decay constants, similar to what we find for the GMM [8,9].

Comparison of the GMM to NL-LSQM shows that these two methods provide estimates with comparable bias and dispersion for larger sample sizes ($N > 20$). However, the GMM shows a moderate advantage in terms of bias at very low sample numbers and does better at estimating the *smaller* of two decay parameters (Fig 6A and 6C) in these cases. The NL-LSQM method often fails to pick out these faster decays when there are very few samples. A partial explanation can be found in the fact that the NL-LSQM method relies on binning, which can be particularly challenging at low counts.

In our test of the GMM on experimental data out to six steps, we found that as we added more steps to the reaction model, the method continued to produce estimates of faster multiple steps. This is not what we found for similar analyses of simulated two-step data, and

suggests that in the experimental system, there are a number of faster steps but that the GMM is not able to determine the exact number of steps nor the rate of each one. The CMM in this case is unable to return real solutions for multiple steps. Fig 7 shows that the slow step is dependent on the protein concentration and that this dwell time decreases as the protein concentration increases. However, the faster steps show little dependence on protein concentration. This could be explained by a mechanism in which the rate limiting step is the site-specific association of the protein with the binding site, followed by a series of faster steps leading to cleavage of one or both DNA strands.

It is important to understand how the GMM compares to current methods of data analysis in molecular biophysics. The majority of these methods have been devised to analyze data from single molecule FRET experiments. In methods such as HMM, assumptions about how the hidden states are connected to the measured signal are made, which allow the time trace of the signal to be interpreted as transitions between molecular states. These methods take as input the experimentally-measured time traces. These detailed data can provide more information on hidden states than exists in a dwell time distribution. For example, multiple FRET efficiencies can aid in the identification of multiple hidden states [3]. Furthermore, recent work has shown that in the case of identical FRET efficiencies of hidden states, methods such as SMACKS [18] and Empirical Bayes [8] can outperform dwell time analysis.

GMM may underperform these methods in the case of analysis of smFRET traces. However, GMM does offer some advantages. As a method of dwell time analysis, it is more broadly applicable, as is shown in our experimental application to a bead loss assay. In addition, it has the ability to be modified to include non-exponential dwell time distributions by modifying the moment functions accordingly. Exponential dwell time distributions are inherent in HMM and related methods. And finally, the GMM is simple to implement, with just a few adjustable parameters. It also is flexible and can be reformulated, requiring only a redefinition of the moment functions. The only requirement is that a sufficient number of moment functions of the measured values and system parameters can be formulated whose expectation values are zero. The number of such moment functions must be at least the number of free parameters in the model.

Supporting information

S1 Supporting Information. Includes all supporting information referred to in the main text. Supporting Information contains all figures, complete results, experimental data, as well as the mathematical proof referred to in the main text.
(PDF)

Acknowledgments

The authors would like to thank Stefano Gambino for his assistance in collecting the experimental data used in this work. This work was funded by the National Science Foundation RUI Award (MCB-1715317) and by Emmanuel College.

Author Contributions

Conceptualization: Allen C. Price.

Funding acquisition: Allen C. Price.

Investigation: Sadie Piatt, Allen C. Price.

Methodology: Allen C. Price.

Software: Allen C. Price.

Writing – original draft: Sadie Piatt, Allen C. Price.

Writing – review & editing: Sadie Piatt, Allen C. Price.

References

1. Bronson JE, Fei J, Hofman JM, Gonzalez RL, Wiggins CH (2009) Learning rates and states from biophysical time series: a Bayesian approach to model selection and single-molecule FRET data. *Biophys J* 97: 3196–3205. <https://doi.org/10.1016/j.bpj.2009.09.031> PMID: 20006957
2. Schröder GF, Grubmüller H (2003) Maximum likelihood trajectories from single molecule fluorescence resonance energy transfer experiments. *J Chem Phys* 119: 9920–9924.
3. Manz C, Kobitski AY, Samanta A, Keller BG, Jäschke A, et al. (2017) Single-molecule FRET reveals the energy landscape of the full-length SAM-I riboswitch. *Nature chemical biology* 13: 1172. <https://doi.org/10.1038/nchembio.2476> PMID: 28920931
4. Maus M, Cotlet M, Hofkens J, Gensch T, De Schryver FC, et al. (2001) An experimental comparison of the maximum likelihood estimation and nonlinear least-squares fluorescence lifetime analysis of single molecules. *Analytical chemistry* 73: 2078–2086. PMID: 11354494
5. Hansen LP (1982) Large sample properties of generalized method of moments estimators. *Econometrica: Journal of the Econometric Society*: 1029–1054.
6. van Oijen AM (2011) Single-molecule approaches to characterizing kinetics of biomolecular interactions. *Current Opinion in Biotechnology* 22: 75–80. <https://doi.org/10.1016/j.copbio.2010.10.002> PMID: 21036593
7. Williams K, Grafe B, Burke KM, Tanner N, van Oijen AM, et al. (2011) A single molecule DNA flow stretching microscope for undergraduates. *American Journal of Physics* 79: 1112–1120.
8. van de Meent J-W, Bronson JE, Wiggins CH, Gonzalez RL Jr (2014) Empirical Bayes methods enable advanced population-level analyses of single-molecule FRET experiments. *Biophys J* 106: 1327–1337. <https://doi.org/10.1016/j.bpj.2013.12.055> PMID: 24655508
9. Chen Y, Shen K, Shan S-O, Kou S (2016) Analyzing single-molecule protein transportation experiments via hierarchical hidden Markov models. *Journal of the American Statistical Association* 111: 951–966. <https://doi.org/10.1080/01621459.2016.1140050> PMID: 28943680
10. Gambino S, Mousley B, Cathcart L, Winship J, Loparo JJ, et al. (2016) A single molecule assay for measuring site-specific DNA cleavage. *Analytical Biochemistry* 495: 3–5. <https://doi.org/10.1016/j.ab.2015.11.013> PMID: 26655389
11. Hansen LP (2010) Generalized method of moments estimation. *Macroeconometrics and Time Series Analysis*: Springer. pp. 105–118.
12. Lück A, Wolf V (2016) Generalized method of moments for estimating parameters of stochastic reaction networks. *BMC systems biology* 10: 98. <https://doi.org/10.1186/s12918-016-0342-8> PMID: 27769280
13. Hall AR (2005) *Generalized method of moments*: Oxford University Press.
14. Floyd DL, Harrison SC, Van Oijen AM (2010) Analysis of kinetic intermediates in single-particle dwell-time distributions. *Biophys J* 99: 360–366. <https://doi.org/10.1016/j.bpj.2010.04.049> PMID: 20643053
15. Zhou Y, Zhuang X (2007) Kinetic analysis of sequential multistep reactions. *The Journal of Physical Chemistry B* 111: 13600–13610. <https://doi.org/10.1021/jp073708+> PMID: 17994718
16. Wishart J (1952) Moment coefficients of the k-statistics in samples from a finite population. *Biometrika* 39: 1–13.
17. Etsen CM, Todorov P, Walt DR (2014) Elucidating Restriction Endonucleases Reaction Mechanisms via Dwell-Time Distribution Analysis. *Biophys J* 106: 22a.
18. Schmid S, Götz M, Hugel T (2016) Single-molecule analysis beyond dwell times: demonstration and assessment in and out of equilibrium. *Biophys J* 111: 1375–1384. <https://doi.org/10.1016/j.bpj.2016.08.023> PMID: 27705761